Impurity density and momentum transport during the sawtooth cycle

C. Marini[1], B. P. Duval[1], L. Federspiel[1], A. N. Karpushov[1], A. Merle[1] and O. Sauter[1]

[1] *Ecole Polytechnique Fédérale de Lausanne (EPFL), Centre de Recherches en Physique des Plasmas (CRPP), CH-1015 Lasusanne, Switzerland*

Introduction

Plasma rotation is one of the open issues in Tokamaks physics, with many phenomena missing a theoretical explanation. Rotation and momentum transport are often observed to be strongly affected by MHD activity, even though their effect is rarely included in theoretical models, and hence must be characterized empirically. Among all the MHD instabilities, the sawtooth instability [1], that is a periodic relaxation of the plasma core pressure, offers an interesting opportunity to examine its effect due to its non destructive nature and reproducibility. Widely accepted reconnection models [2, 3, 4] predict profiles flattening upon sawtooth crash, with particle and energy redistribution up to a mixing radius, which is near the q=1 surface. This paper shows that the effect of the crash on impurities is stronger than this suggests, with observed hollowed density and temperature profiles and unexpected changes in the bulk plasma rotation.

Measurement method

The CXRS diagnostics in TCV routinely provides time resolved Carbon impurity density, temperature and velocity measurements, with a typical time resolution of 20-30 ms and spatial resolution of $\simeq$ 1 cm. Viewlines for the 3 installed CXRS systems are shown in figure (Fig. 1). Each system has 20 x 2 viewlines, arranged in double slit configuration at the spectrometer entrance. Toroidal rotation measurements are performed by the high field side (HFS) and low field side (LFS) systems, while the vertical (VER) system is used for poloidal measurements. The source of neutrals for CX is the diagnostic neutral beam (DNBI), that allows unperturbed measurements thanks to its low power ($\leq$ 80 kW) and hence low applied torque on the plasma (direct torque may be neglected).

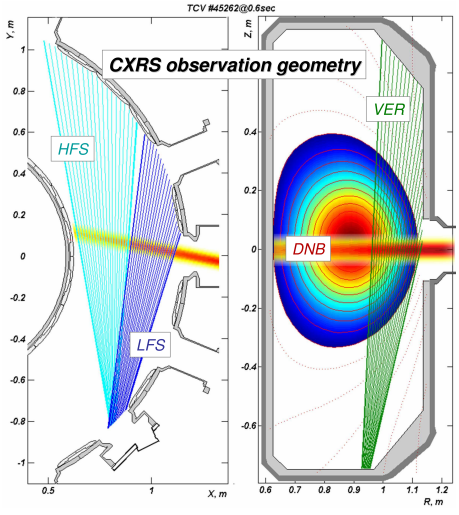

Figure 1: *CXRS viewlines for HFS, LFS and VER systems. DNBI trajectory also shown.*

Time resolved measurements across the sawteeth (ST) events were performed using the LFS system, achieving an integration time of 2 ms and at the same time preserving the high spatial resolution (i.e. $\simeq$1 cm). To overcome

the low photon statistics resulting by the short integration time and low DNBI neutral density, conditionally resampling measurements were employed [5], summing the spectra acquired with the same sawtooth phase, and led to the determination of the properties of a canonical sawtooth (typically averaged over 40 individual ST). For the first time a sawteeth locking technique was successfully employed to obtain CXRS measurements across the entire ST cycle, with a negligible phase shift between different ST. The locking technique exploits sawtooth stabilization [6] by electron cyclotron resonance heating (ECRH) near the q=1 surface, where the crash time can be chosen with a choice of the ECRH power modulation. Data presented here are for TCV discharges #48951 and #48952 that employ a total ECRH power of 375 kW and 460 kW respectively. Since this technique allow the a priori knowledge of each ST crash time, the relative phase of the CXRS acquisition can be set arbitrarily. The synchronization with the DNBI may also be chosen to ensure an optimal ratio between active and passive acquisitions. In these experiments, regular sawteeth of 20 ms period, divided in 10 phases, were studied, for a plasma current of $I_p = -288$ kA and a toroidal magnetic field on axis $B_{\phi 0} = 1.27$ T, chosen to obtain a large ST radius and $q_{edge} \simeq 3$, that is an ITER relevant scenario [4]. A large ST radius, i.e. q=1 surface at $\rho_{q=1} \simeq 0.66$ and inversion radius at $\rho_{inv} \simeq 0.4$, increases the velocity profile resolution in the region of strong MHD activity, together with a weak, although measurable, effect on impurity density and temperature.

Profiles evolution

Similar trends in profile evolutions (Fig. 2) are seen for shots #48951 and #48952. Missing ST phases in both shots (marked with x in the figures legend) are due to a poor choice of CXRS timing that will be corrected in the future. The sign convention for the toroidal velocity shown in figures 2(a) and 2(b) is positive in the co-current direction. Velocity profiles undergo a very fast ($\ll 2$ ms) evolution at the ST crash, with a strong ($\Delta V_i \simeq 20$ km/s) co-current acceleration in the core region, inside ρ_{inv}, that cannot be explained by plasma "mixing" alone requiring an effective co-current momentum source. Simultaneously, a weaker recoil (counter-current acceleration, $\Delta V_i \simeq -5$ km/s) outside ρ_{inv} ensures a partial momentum conservation, that could be ascribed to ST mixing and seems to be confined inside the plasma volume, as the edge velocity values remain fairly constant. The velocity profiles relax continuously during the ST cycle to a fairly monotonic profile, with a positive gradient, and we conclude that a similar profile represents the intrinsic rotation profile in absence of ST activity, as set from turbulent transport. The velocity flattening at $\rho \simeq 0.6$ (i.e. the ECRH deposition radius) is possibly explained by a local increase in transport due to the highly localised additional heating. Averaged profiles, bulged in the co-current direction measured in previous experiments [7], are thus explained by a sudden

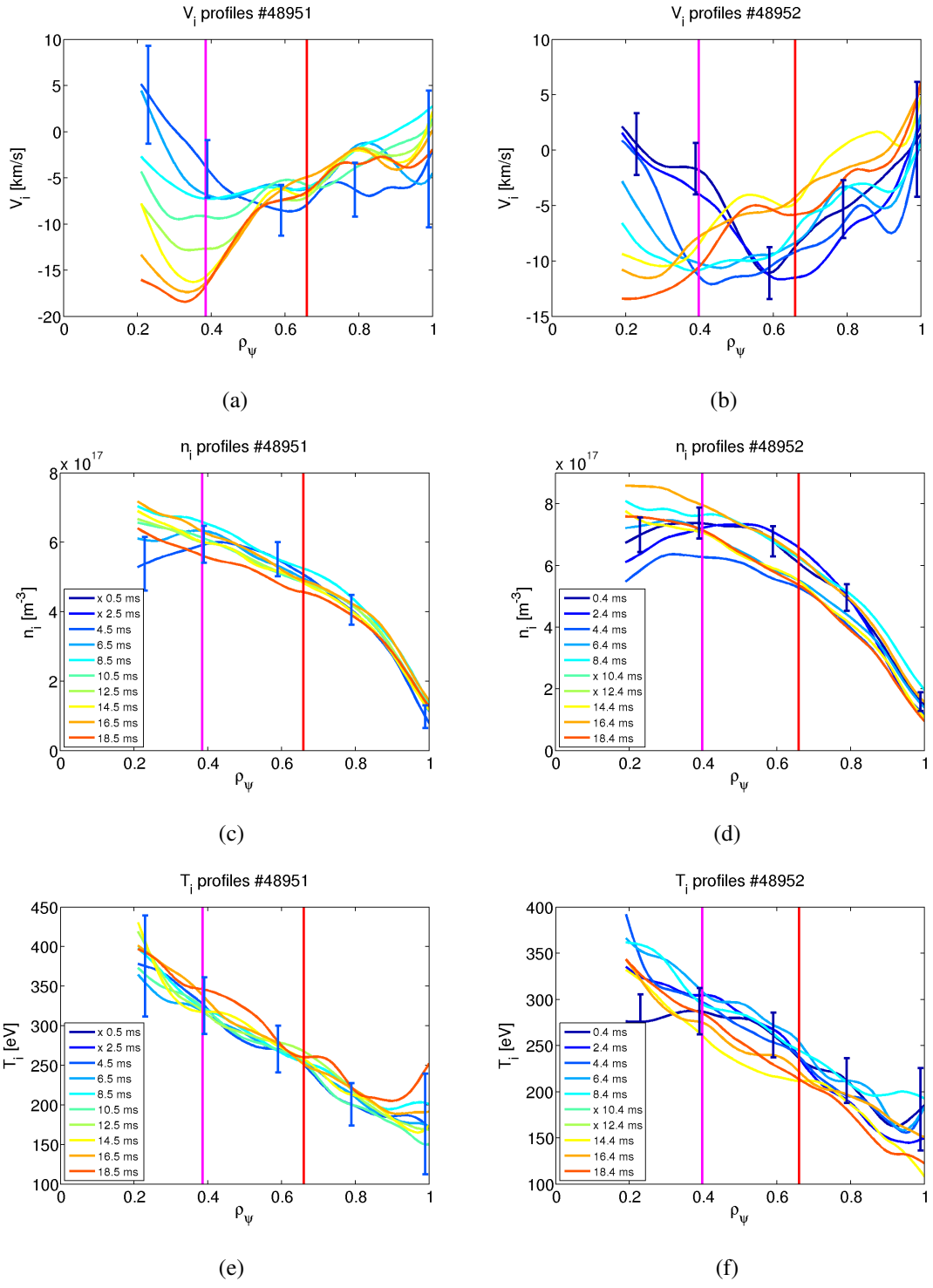

Figure 2: *Time resolved profiles for shots #48951 and #48952. Vertical lines represents* ρ_{inv} *(magenta) and* $\rho_{q=1}$ *(red). Velocity profiles 2(a) and 2(b), a strong and rapid co-current acceleration is evident at the ST crash inside* ρ_{inv}*, with a corresponding recoil outside* ρ_{inv}*, followed by a slow relaxation to a monotonic profile. Density profiles 2(c) and 2(d) are hollowed after the crash and relax in* $\leq$ *7 ms. Temperature profiles 2(e) and 2(f) are hollowed (visible only in 2(f)) and relax in* $<$ *4 ms. Missing profiles phases are marked with x in the figures legend, where the time delay between the midpoint acquisition time and the ST crash is shown.*

jump at the ST crash followed by a slow relaxation to a "natural" condition.

Density profiles (Fig. 2(c) and Fig. 2(d)) after the crash are hollowed inside ρ_{inv} and relax to a peaked profiles on the same timescale ($\simeq$ 7 ms) as the electron density. These are measured by interferometry and Thomson scattering, reconstructed by tomographic inversion, and are also found to be hollow. The impurity density profile has sufficient time to reach a relaxed condition within the ST period, unlike the rotation profile. It's interesting to note that impurities are expelled from the core, so that ST do reduce impurity accumulation. Temperature profile is also hollow, but relaxes on timescales considerably faster than the density and the electron temperature (measured by thomson scattering). This is expected as previous measurements showed a flat averaged density profile and a peaked temperature profile, suggesting different transport mechanisms for particles and energy.

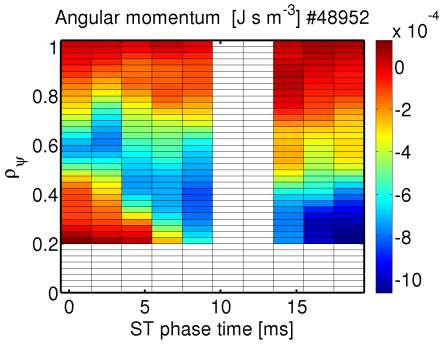

Figure 3: *Surface averaged angular momentum for shot #48952*

The surfaced averaged toroidal angular momentum (Fig. 3) evolution clearly show a co-current acceleration in the core at the crash time, but remaining constant at the LCFS during the whole cycle. The successive phases can be explained by an outward momentum pinch (and/or counter current torque) in the core region and a co-current diffusion/convection from the edge region.

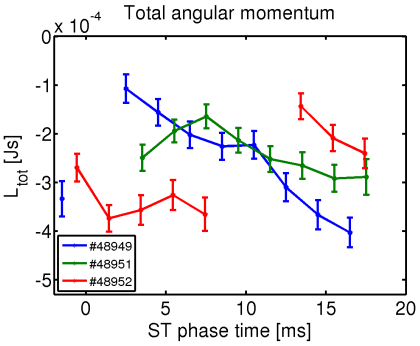

Figure 4: *Total angular momentum evolution for shots 48949, 48951 and 48952*

To date, there is no conclusive evidence for total angular momentum conservation at the ST crash, as shown by the contrasting behaviours for these shots (Fig. 4).

References

[1] S. von Goeler et al., Physics Review Letter, **33** 1201 (1974)

[2] B.B. Kadomtsev, Sov. J. Plasma Phys. **1**, 389 (1975)

[3] J.A. Wesson, Nucl. Fusion **30**, 2545 (1990)

[4] F. Porcelli et al, Plasma Phys. Control. Fusion **38**, 2163 (1996)

[5] F. Felici et al., Fusion Engineering and Design **89**, 165-176 (2014)

[6] G.P. Canal et al., Nuclear Fusion **53**, 113026 (2013)

[7] B.P. Duval et al., Plasma Phys. Control. Fusion **49**, B195 (2007)